

MULTIPLICITY DEPENDENCE OF RESONANCE PRODUCTION WITH ALICE AT THE LHC*

ENRICO FRAGIACOMO

Istituto Nazionale di Fisica Nucleare, Sezione di Trieste, Italy

(Received January 24, 2019)

Particle production in ultra-relativistic heavy-ion collisions at the LHC energies is discussed in the light of the results obtained with ALICE, with special emphasis on the light-flavour hadronic resonances. The most recent measurements from the LHC Run 2, including the Xe–Xe run, are discussed and shown to be in agreement with previous findings.

DOI:10.5506/APhysPolBSupp.12.381

1. Introduction

Hadronic resonances have become suitable tools in the study of bulk particle production in ultra-relativistic heavy-ion collisions, therefore trespassing on their traditional role of probes of the hadronic medium in the late stage of the collision [1]. In this article, a comprehensive set of results obtained with ALICE [2] is presented, encompassing the recent measurements from the LHC Run 2, including the Xe–Xe run. Observables such as particle yield ratios and mean transverse momenta as a function of the charged-particle multiplicity density are shown for $\phi(1020)$ and $K^*(892)$ for all available colliding systems and different collision energies. The comparison with other light-flavour particles offers interesting insights into the understanding of the production mechanisms and the dynamics of the collision. A detailed description of the ALICE apparatus and its performance can be found in Ref. [3].

2. Hadrochemistry of the collision

A remarkable result that has emerged at the LHC energies is that the relative abundances of the particles produced in the collision depend only

* Presented at the XIII Workshop on Particle Correlations and Femtoscopy, Kraków, Poland, May 22–26, 2018.

on the size of the collision system, irrespective whether it is pp , p - A or A - A , and irrespective of the available energy. This holds true for all light-flavour particles, including resonances, as can be deduced from Fig. 1 where a compilation of ratios of particle yields to the pion yield is presented as a function of the charged-particle multiplicity density for pp collisions at $\sqrt{s} = 7$ and 13 TeV, p -Pb collisions at $\sqrt{s_{NN}} = 5.02$ TeV, Pb-Pb collisions at $\sqrt{s_{NN}} = 5.02$ TeV and Xe-Xe collisions at $\sqrt{s_{NN}} = 5.44$ TeV.

For A - A collisions, the charged-particle multiplicity has been proven to be directly related to how large the fireball is at hadronization [4], providing therefore a good indicator for the system size. The new results for Pb-Pb at $\sqrt{s_{NN}} = 5.02$ TeV, Xe-Xe at $\sqrt{s_{NN}} = 5.44$ TeV and pp at $\sqrt{s} = 13$ TeV are also shown in Fig. 1 and confirm the previous findings. The smooth evolution observed when going from low to high multiplicities saturates at values that are well-predicted by statistical hadronization models implementing a grand-canonical approach [5]. For nucleus-nucleus collisions, this is not much surprising, since the yield of most light-flavour hadrons, including light nuclei, can be successfully described by thermal models having only the baryo-chemical potential, the chemical freeze-out temperature and the fireball volume as free parameters [6]. For strange particles, an increasing trend, larger for multi-strange hadrons, is observed from small to large systems. The canonical suppression of strangeness production in small systems, a consequence of local strangeness conservation [7], explains in the context of thermal models the relative enhancement of strangeness production in heavy-ion collisions, historically proposed as a signature of quark-gluon plasma formation [8]. This explanation, however, fails the test

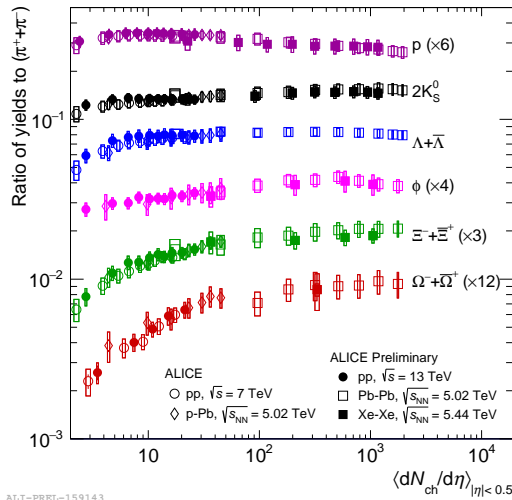


Fig. 1. Ratios of particle yields to the pion yield.

of the ϕ/π ratio. Indeed, for the strangeness-neutral ϕ meson, a flat dependence as a function of the multiplicity is expected, whereas a clear increase by almost a factor two is observed [9].

3. Strangeness production

From Fig. 1, one notes that the ϕ/π ratio increases by an amount similar to that of particles such as the kaon and Λ hyperon, which have total strangeness $S = 1$. This is better observed looking at the ϕ/K ratio in Fig. 2, whose rather flat behaviour is suggestive of a common production mechanism for both the open-strange kaon and the $s\bar{s}$ pair forming the ϕ meson.

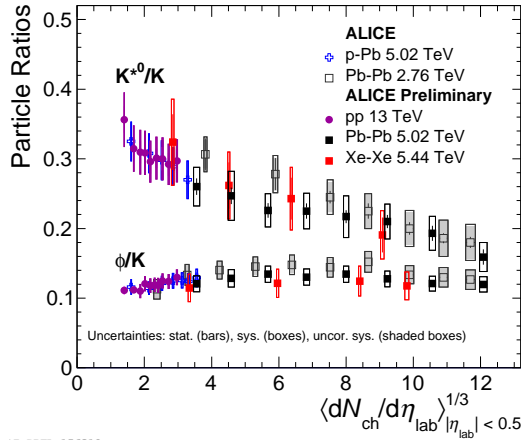


Fig. 2. Ratio of the ϕ and K^{*0} yield to the kaon yield as a function of the charged-particle multiplicity density.

Production mechanisms are hidden in thermal models, which nonetheless fail to predict the flatness of the ϕ/K ratio [10]. In Fig. 2, one would also expect to observe a flat behaviour for the K^{*0}/K ratio, which, contrary to the expectations, presents a significant decrease by almost a factor 2 when going from small to large systems. The new results for Pb–Pb at $\sqrt{s_{NN}} = 5.02$ TeV, Xe–Xe at $\sqrt{s_{NN}} = 5.44$ TeV and pp at $\sqrt{s} = 13$ TeV are in line with earlier results. This decreasing trend, however, is well-understood in terms of the final-state effects in the late hadronic stage of the fireball expansion [11]. Due to its short lifetime, the K^{*0} meson decays during this stage and the decay daughters undergo re-scattering effects that eventually spoil the invariant-mass reconstruction of the resonance. A similar decrease has been observed for other ratios involving resonances, such as ρ/π [12] and Λ^*/Λ [13]. The larger is the volume, as that created in

central nucleus–nucleus collisions, the bigger is the effect. This qualitatively justifies the observed decreasing behaviour of the K^{*0}/K ratio as a function of the multiplicity. Hybrid models implementing transport codes, such as EPOS3 with UrQMD [14], are able to predict the effect. A relatively long hadronic phase has to be assumed: this clearly disfavours models with a kinetic freeze-out immediately following the chemical freeze-out.

4. Average transverse momentum and hydrodynamics

The p_T dependence of particle yields reflects both the different production mechanisms, interplaying at a given p_T , and the collective, hydrodynamical behaviour of the fireball, boosting all particles with the same radial velocity [15].

In order to characterize the transverse momentum spectra, the average transverse momenta $\langle p_T \rangle$ have been evaluated and studied as a function of the system size. This is shown in Fig. 3, where $\langle p_T \rangle$ is plotted as a function of the charged-particle multiplicity density for pions, kaons, protons and ϕ . Two different collision systems (Pb–Pb and Xe–Xe) are compared without observing any significant difference. This result is intriguing since it might indicate that not only the hadrochemistry, as discussed in Sect. 2, but also the spectral shape depends only on the system size. However, hydrodynamical models [16] predict a very small difference in $\langle p_T \rangle$ between Xe–Xe and Pb–Pb, which cannot be resolved by the data. An increasing trend from

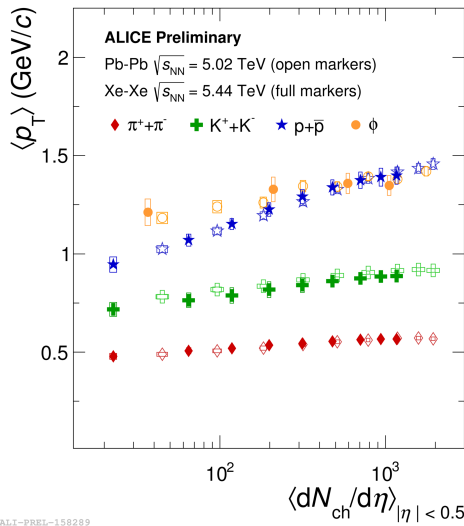


Fig. 3. Average transverse momentum of pion, kaon, proton and ϕ as a function of the charged-particle multiplicity density.

small to large systems is observed for all particles. This increase is smaller for the ϕ meson than for the proton, but in central collisions, the $\langle p_T \rangle$ values of p and ϕ are comparable, in accordance with the mass-scaling law predicted by hydrodynamics for particles with similar mass.

5. Baryon-to-meson ratio

The effect of hydrodynamics which shapes the transverse momentum spectra is further explored studying the baryon-to-meson ratio [17].

This is shown in Fig. 4, where the p/ϕ , p/π and Λ/K_S^0 ratios are plotted as a function of p_T for Pb–Pb and Xe–Xe collisions. The two collision systems give comparable results for centrality classes with similar charged-particle multiplicity density. The flatness of the p/ϕ ratio is consistent with hydrodynamics expectations and it is reproduced by models implementing quark coalescence [18]. The same mechanisms describe the p/π and Λ/K_S^0 ratios, but a substantial radial flow has to be further considered in order to explain the enhancement at intermediate p_T .

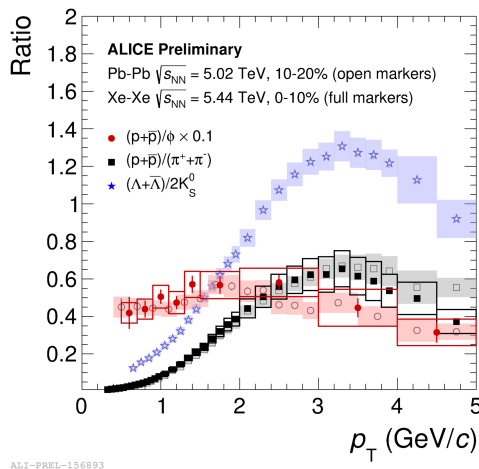


Fig. 4. Baryon-to-meson ratios p/ϕ , p/π and Λ/K_S^0 as a function of p_T for Pb–Pb and Xe–Xe collisions.

6. Conclusions

The recent ALICE results from the LHC Run 2, which includes the Xe–Xe run, confirm previous findings about particle production mechanisms at the LHC energies. The integrated particle ratios depend on the charged-particle multiplicity density in the same way for any colliding system despite crucial differences in the initial states as well as colliding energies. In the

context of thermal models, the smooth evolution from small to large systems finds an explanation that invokes the canonical suppression of strangeness production in small systems. Resonance ratios as ϕ/π , however, seem to escape this picture and remain an important testing bench for particle production models, provided final-state effects in the late hadronic stage of the collision are correctly accounted for. The average transverse momenta as a function of the charged-particle multiplicity density present a different trend for p and ϕ , but converge at a common value, respecting mass scaling. The flatness of the p/ϕ ratio as a function of p_T is also consistent with a hydrodynamical description.

REFERENCES

- [1] G. Torrieri, J. Rafelski, *Phys. Lett. B* **509**, 239 (2001).
- [2] K. Aamodt *et al.* [ALICE Collaboration], *JINST* **3**, S08002 (2008).
- [3] B. Abelev *et al.* [ALICE Collaboration], *Int. J. Mod. Phys. A* **29**, 1430044 (2014).
- [4] K. Aamodt *et al.* [ALICE Collaboration], *Phys. Lett. B* **696**, 328 (2011).
- [5] S. Acharya *et al.* [ALICE Collaboration], *Nucl. Phys. A* **971**, 1 (2018).
- [6] A. Andronic, P. Braun-Munzinger, J. Stachel, *Phys. Lett. B* **673**, 142 (2009).
- [7] K. Redlich, A. Tounsi, *Eur. Phys. J. C* **24**, 589 (2002).
- [8] J. Rafelski, B. Müller, *Phys. Rev. Lett.* **48**, 1066 (1982).
- [9] V. Viskovic, A. Kalweit, [arXiv:1610.03001](https://arxiv.org/abs/1610.03001) [nucl-ex].
- [10] S. Acharya *et al.* [ALICE Collaboration], *Phys. Rev. C* **99**, 024906 (2019) [[arXiv:1807.11321](https://arxiv.org/abs/1807.11321)] [nucl-ex].
- [11] M. Bleicher, J. Aichelin, *Phys. Lett. B* **530**, 81 (2002).
- [12] S. Acharya *et al.* [ALICE Collaboration], [arXiv:1805.04365](https://arxiv.org/abs/1805.04365) [nucl-ex].
- [13] S. Acharya *et al.* [ALICE Collaboration], *Phys. Rev. C* **99**, 024905 (2019) [[arXiv:1805.04361](https://arxiv.org/abs/1805.04361)] [nucl-ex].
- [14] A. Knospe *et al.*, *Phys. Rev. C* **93**, 014911 (2016).
- [15] E. Schnedermann, J. Sollfrank, U. Heinz, *Phys. Rev. C* **48**, 2462 (1993).
- [16] G. Giacalone *et al.*, *Phys. Rev. C* **97**, 034904 (2018).
- [17] F. Bellini, *Nucl. Phys. A* **982**, 427 (2019) [[arXiv:1808.05823](https://arxiv.org/abs/1808.05823)] [nucl-ex].
- [18] V. Minissale, F. Scardina, V. Greco, *Phys. Rev. C* **92**, 054904 (2015).